

# Co-reactant electrogenerated chemiluminescence of iridium(III) complexes containing an acetylacetonate ligand

Lifen Chen,<sup>[a]</sup> Egan H. Doeven,<sup>\*[b]</sup> David J. D. Wilson,<sup>[c]</sup> Emily Kerr,<sup>[a]</sup> David J. Hayne,<sup>[a]</sup> Conor F. Hogan,<sup>[c]</sup> Wenrong Yang,<sup>[a]</sup> Tien T. Pham,<sup>[a]</sup> and Paul S. Francis<sup>\*[a]</sup>

**Abstract:** We examine the electrogenerated chemiluminescence (ECL) of three  $\text{Ir}(\text{C}^{\wedge}\text{N})_2(\text{acac})$  complexes, where  $\text{acac}$  = acetylacetonate anion and  $\text{C}^{\wedge}\text{N}$  = 2-phenylpyridine (ppy), 2-phenylbenzothiazole (bt) or 2-phenylquinoline (pq) anions, with tri-*n*-propylamine co-reactant in acetonitrile, under a range of chemical and instrumental conditions, following somewhat conflicting recent claims of the ECL intensities from complexes of this type. Relevant electrochemical, spectroscopic and ECL properties are evaluated in direct comparison with those of  $\text{Ir}(\text{ppy})_3$  and  $[\text{Ru}(\text{bpy})_3](\text{PF}_6)_2$ , and data from previous publications. DFT calculations on the  $\text{Ir}(\text{C}^{\wedge}\text{N})_2(\text{acac})$  complexes show the HOMOs to be composed of both the metal and  $\text{C}^{\wedge}\text{N}$  ligand, and LUMOs almost exclusively on the  $\text{C}^{\wedge}\text{N}$  ligand. The ECL intensities of the  $\text{Ir}(\text{C}^{\wedge}\text{N})_2(\text{acac})$  complexes (relative to  $[\text{Ru}(\text{bpy})_3](\text{PF}_6)_2$ ) were dependent on experimental conditions, and in some cases, the ECL intensities reported for iridium complexes may have been derived using conditions that unintentionally disadvantaged the reference electrochemilumiphore.

## Introduction

After the success of ruthenium(II) bipyridine complexes as electrogenerated chemiluminescence (ECL) reagents,<sup>[1]</sup> researchers began to examine a range of cyclometalated iridium(III) complexes exhibiting high photoluminescence efficiencies and a wide range of emission wavelengths, seeking advances in detection sensitivity<sup>[2]</sup> and multi-colour (multiplexed) detection systems.<sup>[3]</sup>

Initial demonstrations of ECL reactions involving homoleptic  $\text{Ir}(\text{ppy})_3$  (ppy = 2-phenylpyridine anion) were promising.<sup>[3a, 4]</sup> Kapturkiewicz and co-workers then examined a series of heteroleptic iridium(III) complexes containing an acetylacetonate anion (acac) ligand, such as  $\text{Ir}(\text{ppy})_2(\text{acac})$  and  $\text{Ir}(\text{bt})_2(\text{acac})$ , where bt = 2-phenylbenzothiazole anion (Figure 1).<sup>[5]</sup> Like  $\text{Ir}(\text{ppy})_3$ , these complexes exhibited high photoluminescence efficiencies and had previously been employed as electroluminescence phosphors in organic light emitting devices.<sup>[6]</sup>

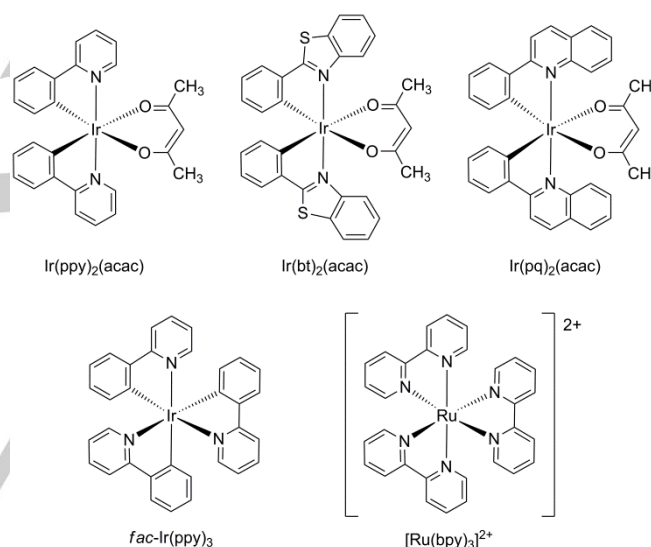


**Figure 1.**  $\text{Ir}(\text{ppy})_2(\text{acac})$ : bis(2-phenylpyridine)(acetylacetonato)iridium(III);  $\text{Ir}(\text{bt})_2(\text{acac})$ : bis(2-phenylbenzothiazole)(acetylacetonato)iridium(III);  $\text{Ir}(\text{pq})_2(\text{acac})$ : bis(2-phenylquinoline)(acetylacetonato)iridium(III);  $\text{fac-Ir}(\text{ppy})_3$ : fac-tris(2-phenylpyridine)iridium(III);  $[\text{Ru}(\text{bpy})_3]^{2+}$ : tris(2,2'-bipyridine)ruthenium(II).

Kapturkiewicz *et al.* observed impressive ECL efficiencies ( $\phi_{\text{ECL}}$  up to 0.55) when using the triple-potential-step technique to generate the oxidised  $[\text{Ir}(\text{C}^{\wedge}\text{N})_2(\text{acac})]^+$  complex and the reduced radical anions of aromatic nitriles in 1:1 acetonitrile-dioxane,<sup>[5]</sup> compared to the self-annihilation of tris(2,2'-bipyridine)ruthenium(II) ( $[\text{Ru}(\text{bpy})_3]^{2+}$ ) in acetonitrile ( $\phi_{\text{ECL}}$  = 0.05).<sup>[7]</sup> Around the same time, Kim *et al.*<sup>[2a]</sup> identified  $\text{Ir}(\text{pq})_2(\text{acac})$  and  $\text{Ir}(\text{pq})_2(\text{tmd})$  (pq = 2-phenylquinoline anion, tmd = 2,2',6,6'-tetramethylhepta-3,5-dione anion) as fulfilling two parameters essential for efficient co-reactant ECL with tri-*n*-propylamine (TPrA), considering the detailed ECL mechanism for  $[\text{Ru}(\text{bpy})_3]^{2+}$  and TPrA outlined by Bard and co-workers (Eqn 1-9),<sup>[8]</sup> where  $\text{TPrA}^{+}$  is the corresponding aminium radical cation ( $\text{Pr}_3\text{N}^{+}$ ) and  $\text{TPrA}^{\cdot}$  is an  $\alpha$ -amino alkyl radical ( $\text{Pr}_2\text{NCH}^{\cdot}\text{CH}_2\text{CH}_3$ ).

[a] Ms L. Chen, Ms E. Kerr, Dr D.J. Hayne, Dr W. Yang, Ms T.T. Pham and Prof. P.S. Francis\*

Centre for Chemistry and Biotechnology, School of Life and Environmental Sciences, Faculty of Science, Engineering and Built Environment, Deakin University, Waurn Ponds, Victoria 3216, Australia.

E-mail: paul.francis@deakin.edu.au

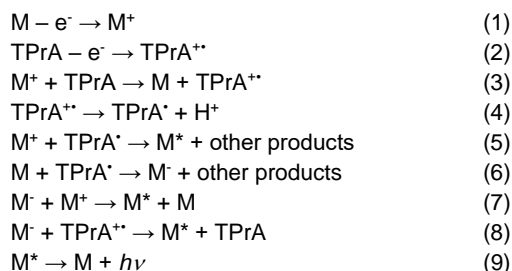
[b] Dr E.H. Doeven\*

Centre for Regional and Rural Futures (CeRRF), Faculty of Science, Engineering and Built Environment, Deakin University, Waurn Ponds, Victoria 3216, Australia.

Email: egan.doeven@deakin.edu.au

[c] Dr D.J.D. Wilson and A/Prof. C.F. Hogan

Department of Chemistry and Physics, La Trobe Institute for Molecular Science, La Trobe University, Melbourne, Victoria 3086, Australia.



Kim *et al.*<sup>[2a]</sup> recorded relative co-reactant ECL efficiencies<sup>§</sup> for Ir(pq)<sub>2</sub>(acac) and Ir(pq)<sub>2</sub>(tmd) (with TPrA in acetonitrile) that were 77-fold and 49-fold greater than that of [Ru(bpy)<sub>3</sub>]<sup>2+</sup>, respectively. They attributed the enhancement to the suitability of their respective redox potentials for fast generation of TPrA<sup>++</sup> via Eqn 3, and the efficient acceptance of electrons from TPrA<sup>+</sup> in Eqn 6. In a closely related subsequent investigation, Zhou *et al.*<sup>[9]</sup> reported that the ECL signals for Ir(pq)<sub>2</sub>(acac) and Ir(pq)<sub>2</sub>(dm-acac) with TPrA co-reactant in acetonitrile were 10-fold and 38-fold greater than that of [Ru(bpy)<sub>3</sub>]<sup>2+</sup>, under identical conditions.<sup>†</sup> An even greater relative co-reactant ECL intensity (214-fold of that of [Ru(bpy)<sub>3</sub>]<sup>2+</sup>) was observed for Ir(bt)<sub>2</sub>(acac) with TPrA in dichloromethane,<sup>[10]</sup> but unlike the previous studies,<sup>[2a, 9]</sup> their relative ECL intensities in acetonitrile were not reported.

These extraordinary ECL intensities with TPrA as co-reactant (relative to the conventional ruthenium(II) complex luminophore that is employed in commercial ECL-based immunodiagnostics systems) promise superior detection sensitivity and multi-colour detection techniques. However, Kapturkiewicz<sup>[2f]</sup> has questioned the validity of the prior, somewhat conflicting evaluations of the relative ECL intensities of these iridium complexes. Moreover, Fernandez-Hernandez *et al.*<sup>[11]</sup> recently reported a much lower relative co-reactant ECL for Ir(pq)<sub>2</sub>(acac) of 0.11 (vs [Ru(bpy)<sub>3</sub>]<sup>2+</sup> = 1) under aqueous conditions.

With these considerations in mind, we have re-examined several promising electrochemiluminophores (Ir(ppy)<sub>2</sub>(acac), Ir(bt)<sub>2</sub>(acac) and Ir(pq)<sub>2</sub>(acac)),<sup>[5, 9–10]</sup> in direct comparison with the archetypal [Ru(bpy)<sub>3</sub>]<sup>2+</sup> and Ir(ppy)<sub>3</sub> complexes. We evaluate the relative ECL intensities of these complexes with TPrA co-reactant in acetonitrile across a range of complex and co-reactant concentrations, and instrument configurations. These experiments not only reconcile some wide discrepancies between previously reported data, but also reveal several major shortcomings of conventional approaches to evaluate ECL luminophore candidates.

## Results and Discussion

### Spectroscopic properties

The UV-visible absorption spectra of the Ir(C<sup>N</sup>)<sub>2</sub>(acac) complexes (Figure 2a) were in good agreement with previous reports,<sup>[10, 12]</sup> in which the intense absorption bands between 250 nm and 350 nm were assigned to spin-allowed singlet intra-ligand (<sup>1</sup>LC) transitions ( $\pi \rightarrow \pi^*$ , ppy/bt/pq) and the weaker bands above

400 nm to mixed singlet and triplet metal-to-ligand charge-transfer (MLCT) transitions ( $d\pi(\text{Ir}) \rightarrow \pi^*(\text{ppy/bt/pq})$ ) and intra-ligand transitions.<sup>[12a, 12b]</sup>

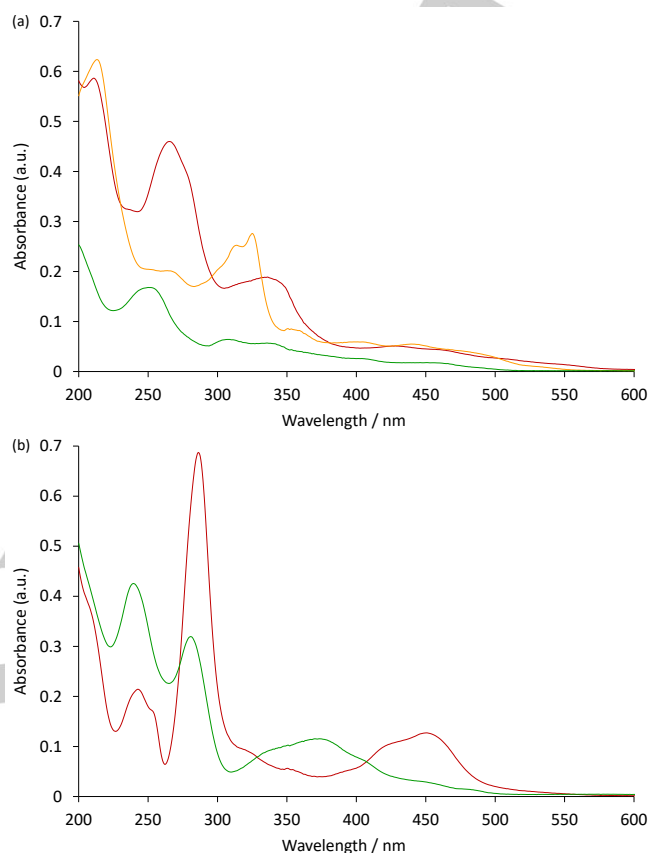


**Figure 2.** Absorption spectra of (a) Ir(ppy)<sub>2</sub>(acac) (green line), Ir(bt)<sub>2</sub>(acac) (yellow line), Ir(pq)<sub>2</sub>(acac) (red line), and (b) Ir(ppy)<sub>3</sub> (green line), and [Ru(bpy)<sub>3</sub>]<sup>2+</sup> (red line), at 10  $\mu\text{M}$  in acetonitrile.

The photoluminescence emission spectra of the Ir(C<sup>N</sup>)<sub>2</sub>(acac) complexes in acetonitrile each exhibited a broad band (Figure 3a) with a maximum intensity at 525, 565 and 611 nm for Ir(ppy)<sub>2</sub>(acac), Ir(bt)<sub>2</sub>(acac) and Ir(pq)<sub>2</sub>(acac), respectively. The luminescence of these complexes has previously been attributed to mixed <sup>3</sup>LC ( $\pi \rightarrow \pi^*$ ) and <sup>3</sup>MLCT ( $d\pi(\text{Ir}) \rightarrow \pi^*(\text{ppy/bt/pq})$ ) transitions.<sup>[12a]</sup> The vibronic fine structure of Ir(bt)<sub>2</sub>(acac), with a pronounced shoulder at ~600 nm, suggests a significant ligand <sup>3</sup>( $\pi \rightarrow \pi^*$ ) contribution in that case.

As shown in Table 1, the luminescence properties of Ir(bt)<sub>2</sub>(acac) are somewhat intermediate to those of Ir(ppy)<sub>2</sub>(acac) and Ir(pq)<sub>2</sub>(acac), and also to those of Ir(ppy)<sub>3</sub> and [Ru(bpy)<sub>3</sub>]<sup>2+</sup>. The maximum emission wavelengths of these complexes increase in the order: Ir(ppy)<sub>3</sub> < Ir(ppy)<sub>2</sub>(acac) << Ir(bt)<sub>2</sub>(acac) << Ir(pq)<sub>2</sub>(acac) < [Ru(bpy)<sub>3</sub>]<sup>2+</sup>, which is seen in their application as luminophores in green (Ir(ppy)<sub>3</sub> and Ir(ppy)<sub>2</sub>(acac)), yellow (Ir(bt)<sub>2</sub>(acac)) and orange-red (Ir(pq)<sub>2</sub>(acac) and [Ru(bpy)<sub>3</sub>]<sup>2+</sup>) light-emitting devices.<sup>[6, 13]</sup> There is considerable variation in the wavelengths of maximum photoluminescence intensity ( $\lambda_{\text{max}}$ )

reported in the literature (Table 1). The emission bands are broad, exhibiting widths at half peak height ( $W_{1/2}$ ) of 77–119 nm, and thus the maxima are vulnerable to error from small changes arising from solvent effects<sup>[3a, 14]</sup> and instrumental noise and intensity fluctuations. Moreover, significant error is introduced by the difference in the sensitivity of the instrument across the wavelength range (Figures S1–S5 in ESI), which is commonly left uncorrected. As the sensitivity of typical photomultiplier tubes decreases sharply into near-infrared region, this effect is most pronounced on luminophores with intensity maxima at the red end of the visible region, such as  $\text{Ir}(\text{pq})_2(\text{acac})$  and  $[\text{Ru}(\text{bpy})_3]^{2+}$ . With our spectrometer, correction for this artefact resulted in changes in  $\lambda_{\text{max}}$  of up to 11 nm, and our corrected values were in good agreement with previously reported corrected values in the same solvent.<sup>[11, 14–15]</sup>

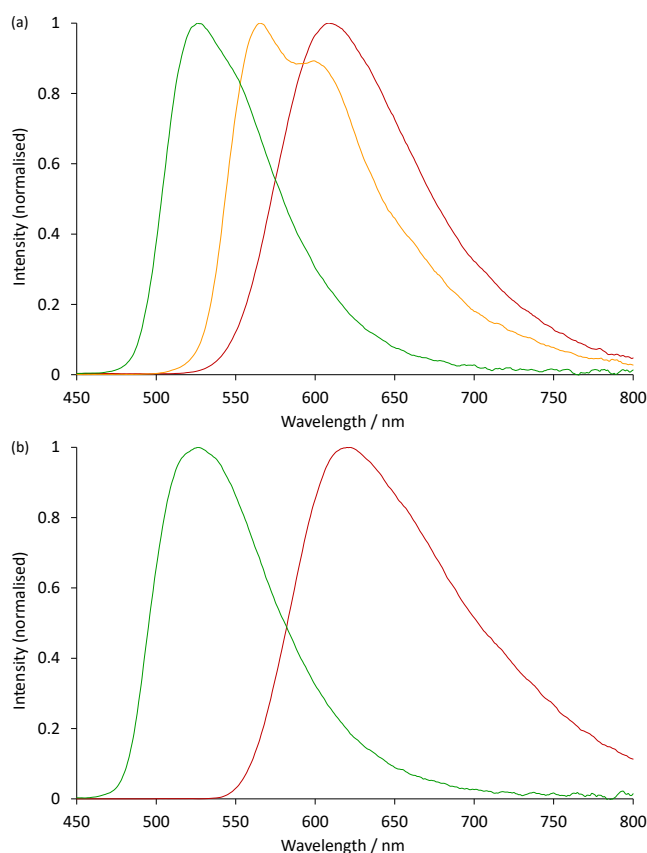


**Figure 3.** Corrected room-temperature photoluminescence emission spectra of (a)  $\text{Ir}(\text{ppy})_2(\text{acac})$  (green line),  $\text{Ir}(\text{bt})_2(\text{acac})$  (yellow line),  $\text{Ir}(\text{pq})_2(\text{acac})$  (red line), and (b)  $\text{Ir}(\text{ppy})_3$  (green line), and  $[\text{Ru}(\text{bpy})_3]^{2+}$  (red line), at 10  $\mu\text{M}$  in acetonitrile. An excitation wavelength of 350 nm was used for all complexes except  $[\text{Ru}(\text{bpy})_3]^{2+}$ , for which 450 nm was used. See also: Figures S1–S5.

Correction of spectra obtained at 77 K in 4:1 (v/v) ethanol:methanol had a much smaller effect on their  $\lambda_{\text{max}}$ , because the emission bands were narrower, although the intensity ratio of the multiple bands within each spectrum was significantly altered (Figure 4 and S1–S5). Our measurements of  $\lambda_{\text{max}}$  for  $\text{Ir}(\text{ppy})_3$  were within 2 nm of those previously reported by

Dedeian *et al.*,<sup>[16]</sup> Nakamaru *et al.*,<sup>[17]</sup> and Djurovich *et al.*<sup>[18]</sup> (Table 1), despite differences in solvent and/or counter ion, with the exception of  $\text{Ir}(\text{pq})_2(\text{acac})$ , for which we obtained 581 nm in 4:1 (v/v) ethanol:methanol, whereas Djurovich *et al.* reported 575 nm in 2-methyltetrahydrofuran (2-MeTHF). Frey *et al.*<sup>[12c]</sup> recently observed the  $\lambda_{\text{max}}$  of  $\text{Ir}(\text{ppy})_2(\text{acac})$  in 2-MeTHF at 77 K as 506 nm, but our result (501 nm) was in better agreement with that of Djurovich *et al.*<sup>[18]</sup> (500 nm) in the same solvent.

The reported photoluminescence quantum efficiencies ( $\phi_{\text{PL}}$ ) of the  $\text{Ir}(\text{C}^{\wedge}\text{N})_2(\text{acac})$  complexes in deaerated solutions vary widely (Table 1), but when compared under the same conditions within a single study,<sup>[12a]</sup> they decrease in the order  $\text{Ir}(\text{ppy})_2(\text{acac}) > \text{Ir}(\text{bt})_2(\text{acac}) > \text{Ir}(\text{pq})_2(\text{acac})$ . In general, the  $\phi_{\text{PL}}$  of the  $\text{Ir}(\text{C}^{\wedge}\text{N})_2(\text{acac})$  complexes are lower than that of  $\text{Ir}(\text{ppy})_3$ , but much higher than that of  $[\text{Ru}(\text{bpy})_3]^{2+}$ . However, in air-equilibrated solutions, the difference is off-set by the greater susceptibility of the electronically excited iridium complexes to oxygen quenching.<sup>[18]</sup> The  $\phi_{\text{PL}}$  of  $\text{Ir}(\text{bt})_2(\text{acac})$  in aerated acetonitrile at room temperature (0.016),<sup>[12b]</sup> for example, is similar to that of  $[\text{Ru}(\text{bpy})_3]^{2+}$  (0.018).<sup>[14]</sup>

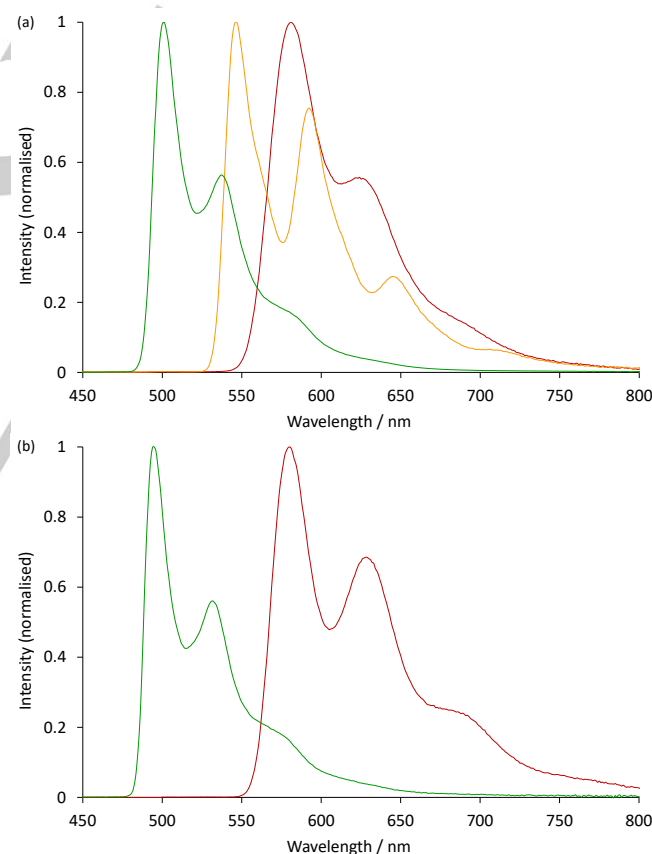


**Figure 4.** Corrected low-temperature (77 K) photoluminescence emission spectra of (a)  $\text{Ir}(\text{ppy})_2(\text{acac})$  (green line),  $\text{Ir}(\text{bt})_2(\text{acac})$  (yellow line),  $\text{Ir}(\text{pq})_2(\text{acac})$  (red line), and (b)  $\text{Ir}(\text{ppy})_3$  (green line), and  $[\text{Ru}(\text{bpy})_3]^{2+}$  (red line), at 5  $\mu\text{M}$  in 4:1 (v/v) ethanol:methanol. See also: Figures S1–S5.

**Table 1.** Selected spectroscopic and electrochemical data for the Ir(C<sup>N</sup>)<sub>2</sub>(acac) complexes in comparison with those of fac-Ir(ppy)<sub>3</sub> and [Ru(bpy)<sub>3</sub>](PF<sub>6</sub>)<sub>2</sub>

	Ir(ppy) <sub>3</sub>	Ir(ppy) <sub>2</sub> (acac)	Ir(bt) <sub>2</sub> (acac)	Ir(pq) <sub>2</sub> (acac)	[Ru(bpy) <sub>3</sub> ] <sup>2+</sup>
<b>Photoluminescence</b>					
Emission colour	Green	Green	Yellow	Orange-Red	Orange-Red
λ <sub>max</sub> /nm (298 K)	510 <sup>[2a]</sup> 514 (toluene) <sup>[19]</sup> 517 (ACN) <sup>[3a]</sup> 520 (ACN) <sup>[15]</sup>	516 (2-MeTHF) <sup>[12a]</sup> 517 (DCM) <sup>[20]</sup> 526 (ACN-DX) <sup>[5b]</sup> 528 (ACN) <sup>[12c]</sup>	557 (2-MeTHF) <sup>[12a]</sup> 557, 590 sh (DCM) <sup>[12b]</sup> 563, 603 sh (ACN) <sup>[12b]</sup> 566 (ACN-DX) <sup>[5b]</sup>	589 <sup>[2a]</sup> 597 (2-MeTHF) <sup>[12a]</sup> 600 (DCM) <sup>[21]</sup> 604 (ACN) <sup>[9]</sup> 612 (ACN) <sup>[11]</sup>	608 <sup>[2a]</sup> 615 (ACN) <sup>[22]</sup> 621 (ACN) <sup>[14]</sup> 625 (H <sub>2</sub> O) <sup>[14]</sup>
φ <sub>PL</sub> (298 K, deaerated)	0.40 (DCM) <sup>[2a]</sup> 0.70 (ACN) <sup>[4c]</sup> 0.89 (DCE) <sup>[23]</sup> 0.90 (DCM) <sup>[24]</sup> 0.97 (2-MeTHF) <sup>[25]</sup>	0.11 (DCM) <sup>[9]</sup> 0.34 (2-MeTHF) <sup>[12a]</sup> 0.53 (DCM) <sup>[20]</sup> 0.72 (ACN-DX) <sup>[5b]</sup>	0.22 (DCM) <sup>[10]</sup> 0.26 (2-MeTHF) <sup>[12a]</sup> 0.44 (ACN-DX) <sup>[5a]</sup>	0.10 (2-MeTHF) <sup>[12a]</sup> 0.10 (DCM) <sup>[2a]</sup> 0.59 (ACN) <sup>[11]</sup> 0.60 (ACN) <sup>[9]</sup> 0.70 (DCE) <sup>[23]</sup>	0.063 (H <sub>2</sub> O) <sup>[14]</sup> 0.095 (ACN) <sup>[14]</sup>
τ/μsec (298 K, deaerated)	1.6 (DCM) <sup>[24]</sup> 1.9 (ACN) <sup>[16]</sup> 2.0 (toluene) <sup>[19]</sup>	1.43 (toluene) <sup>[18]</sup> 1.6 (2-MeTHF) <sup>[12a]</sup> 2.4 (DCM) <sup>[9]</sup>	1.41 (toluene) <sup>[18]</sup> 1.8 (2-MeTHF) <sup>[12a]</sup> 2.0 (DCM) <sup>[10]</sup>	1.50 (toluene) <sup>[18]</sup> 2.0 (2-MeTHF) <sup>[12a]</sup> 1.8 (ACN) <sup>[11]</sup>	0.65 (H <sub>2</sub> O) <sup>[17]</sup> 0.89 (ACN) <sup>[17]</sup> 1.10 (ACN) <sup>[22]</sup>
λ <sub>max</sub> /nm (77 K)	494 (EtOH-MeOH) <sup>[16]</sup>	500 (2-MeTHF) <sup>[18]</sup> 506 (2-MeTHF) <sup>[12c]</sup>	544 (2-MeTHF) <sup>[18]</sup>	575 (2-MeTHF) <sup>[18]</sup>	582, 629 (EtOH-MeOH) <sup>[17]</sup> 582 (EtOH-MeOH) <sup>[22]</sup> 5.1 (EtOH-MeOH) <sup>[17]</sup>
τ/μsec (77 K)	5.0 (EtOH-MeOH) <sup>[26]</sup>	3.2 (DCM) <sup>[12a]</sup>	4.4 (2-MeTHF) <sup>[12a]</sup>		
E <sub>0-0</sub> /eV	2.49 <sup>[19]</sup>	2.48 <sup>[18]</sup>	2.28 <sup>[18]</sup>	2.16 <sup>[18]</sup>	2.12 <sup>[8]</sup> , 2.13 <sup>[22]</sup>
<b>Electrochemistry</b>					
E <sup>0</sup> <sub>ox</sub> /V vs Fc <sup>0/+</sup>	0.31 (ACN-DX) <sup>[4c]</sup> 0.32 <sup>[27]</sup> 0.33 (ACN) <sup>[2e]</sup> 0.36 (ACN) <sup>[16]</sup> 0.44 (ACN) <sup>[2a]</sup>	0.34 (DCM) <sup>[10]</sup> 0.40 (ACN-DX) <sup>[5b]</sup> 0.41 (DMF) <sup>[12c]</sup>	0.50 (DCM) <sup>[10]</sup> 0.56 (ACN) <sup>[12b]</sup> 0.57 (ACN-DX) <sup>[5b]</sup>	0.47 (ACN) <sup>[11]</sup> 0.53 (ACN) <sup>[9]</sup> 0.56 (ACN) <sup>[2a]</sup> 0.57 (ACN) <sup>[28]</sup> 0.64 (DCM) <sup>[21]</sup>	0.89 (ACN) <sup>[29]</sup> 0.93 (ACN) <sup>[2a]</sup> 0.97 (ACN) <sup>[30]</sup>
E <sup>0</sup> <sub>red</sub> /V vs Fc <sup>0/+</sup>	-2.62 (ACN) <sup>[2a]</sup> -2.67 (ACN) <sup>[2e]</sup> -2.69 <sup>[27]</sup> -2.70, -2.95 (ACN-DX) <sup>[4c]</sup>	-2.60 (DMF) <sup>[12c]</sup> -2.61 <sup>[27]</sup>	-2.29 <sup>[27]</sup> -2.63 (THF) <sup>[10]</sup>	-2.05 (ACN) <sup>[2a, 28]</sup> -2.11 (ACN) <sup>[11]</sup> -2.24 (ACN) <sup>[9]</sup> -2.52 (THF) <sup>[21]</sup>	-1.71, -1.90, -2.14 (ACN) <sup>[30]</sup> -1.75, -1.93, -2.18 (ACN) <sup>[29]</sup> -1.75 (ACN) <sup>[2a]</sup>
ΔE/V	3.00 <sup>[2e]</sup> 3.01 <sup>[27]</sup>	3.01 <sup>[12c, 27]</sup>	2.85 <sup>[27]</sup> 3.13 <sup>[10]</sup>	2.58 <sup>[11]</sup> 2.62 <sup>[28]</sup> 2.77 <sup>[9]</sup>	2.65 <sup>[29]</sup> 2.68 <sup>[2a, 30]</sup>
<b>Electrochemiluminescence</b>					
φ <sub>ECL</sub> (annihilation)	0.14 (ACN) <sup>[4b]</sup> 0.16 (ACN-DX) <sup>[4c]</sup>	-	-	0.16 (ACN) <sup>[28]</sup>	0.050 (ACN) <sup>[7]</sup>
φ <sub>ECL</sub> (organic radical anions)	0.67 (with 2-cyanofluorene in ACN-DX) <sup>[4c]</sup>	0.55 (with 4,4'-dicyano-p-biphenyl in ACN-DX) <sup>[5b]</sup>	0.32 (with 1,4-dicyanobenzene in ACN-DX) <sup>[5a]</sup>	0.20 for closely related structural isomer Ir(piq) <sub>2</sub> (acac) (with 1,4-dicyanobenzene in ACN-DX) <sup>[5b]</sup>	0.021 (with 9,10-anthraquinone in ACN) <sup>[31]</sup>
Relative intensity with TPRA as co-reactant <sup>§</sup> (I <sub>0</sub> /I <sub>rel</sub> )	0.0044 (ACN-H <sub>2</sub> O 1:1) <sup>[3a]</sup> 0.014 (ACN) <sup>[2e]</sup> 0.33 (ACN) <sup>[3a]</sup>	0.96 (DCM) <sup>[10]</sup>	214 (DCM) <sup>[10]</sup>	0.1 (H <sub>2</sub> O) <sup>[11]</sup> 10 (ACN) <sup>[9]</sup> 77 (ACN) <sup>[2a]</sup>	1 (by definition <sup>§</sup> )

The φ<sub>PL</sub> is an important consideration in the exploration of new ECL luminophores. The φ<sub>ECL</sub> is the product of the efficiencies of excitation to the excited state (φ<sub>ex</sub>) and the subsequent

luminescence (φ<sub>em</sub>), the latter being equivalent to the φ<sub>PL</sub>. Thus, in an ECL system where the excitation efficiency is very high, the φ<sub>ECL</sub> will approach the φ<sub>PL</sub> limit. This can be seen in the φ<sub>ECL</sub> of



systems in which these complexes are oxidised in conjunction with the reduction of certain aromatic nitriles and ketones (see Table 1, second last row).<sup>[4c, 5b, 31]</sup> Considering that the upper estimate of the  $\phi_{PL}$  of  $\text{Ir}(\text{bt})_2(\text{acac})$  <sup>[5a]</sup> is less than 5-fold the  $\phi_{PL}$  of  $[\text{Ru}(\text{bpy})_3]^{2+}$ ,<sup>[14]</sup> and if we assume that under identical conditions, the relative ECL intensity is approximately equal to the co-reactant ECL efficiency,<sup>§</sup> then the claimed relative ECL of 214 for  $\text{Ir}(\text{bt})_2(\text{acac})$  with TPRA ( $[\text{Ru}(\text{bpy})_3]^{2+} = 1$ )<sup>[10]</sup> would require more than 40-fold greater efficiency in the co-reactant excitation process ( $\phi_{ex}$ ) for the  $\text{Ir}(\text{bt})_2(\text{acac})$  complex compared to  $[\text{Ru}(\text{bpy})_3]^{2+}$ .

### Electrochemistry

In their examination of the co-reactant ECL of  $\text{Ir}(\text{bt})_2(\text{acac})$ , Zhou *et al.*<sup>[10]</sup> initially attempted to characterise the electrochemical potentials of the complexes in dichloromethane with 0.1 M TBAPF<sub>6</sub> as the supporting electrolyte. Under these conditions, a reversible oxidation (0.50 V vs  $\text{Fc}^{0/+}$ ) was observed, but an alternative solvent (tetrahydrofuran) with a more negative working potential range was required to detect the reduction peak (-2.63 vs  $\text{Fc}^{0/+}$ ). However, this potential gap ( $\Delta E = 3.13$  V) is much larger than that reported for related iridium(III) complexes exhibiting higher energy emissions, such as  $\text{Ir}(\text{ppy})_3$ ,<sup>[2e, 27]</sup> and  $\text{Ir}(\text{ppy})_2(\text{acac})$ .<sup>[12c, 27]</sup> (Table 1). Using acetonitrile as a solvent (with 0.1 M TBAPF<sub>6</sub> as the supporting electrolyte), we observed reversible oxidation and reduction peaks at 0.58 V and -2.24 V vs  $\text{Fc}^{0/+}$  (Figure 5). These values are similar those reported by Chen *et al.*<sup>[27]</sup> and provide a more reasonable  $\Delta E$  of 2.82 V.

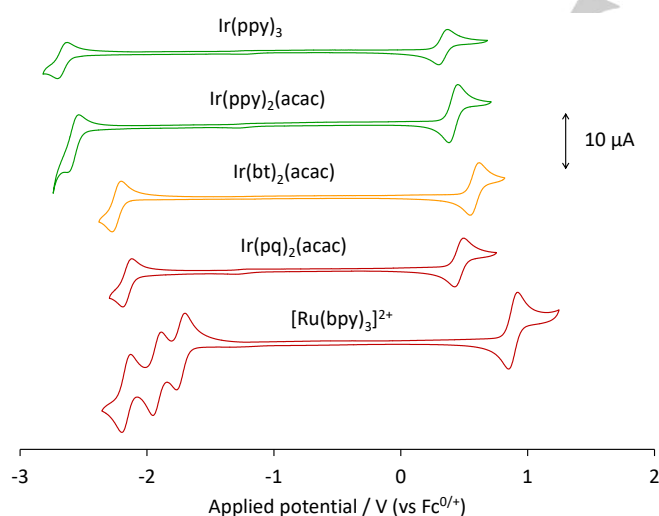


**Figure 5.** Cyclic voltammetry of the five complexes at 0.25 mM in acetonitrile with 0.1 M TBAPF<sub>6</sub>, using a scan rate of 0.1 V s<sup>-1</sup>. The voltammograms have been off-set on the y-axis for clarity only.

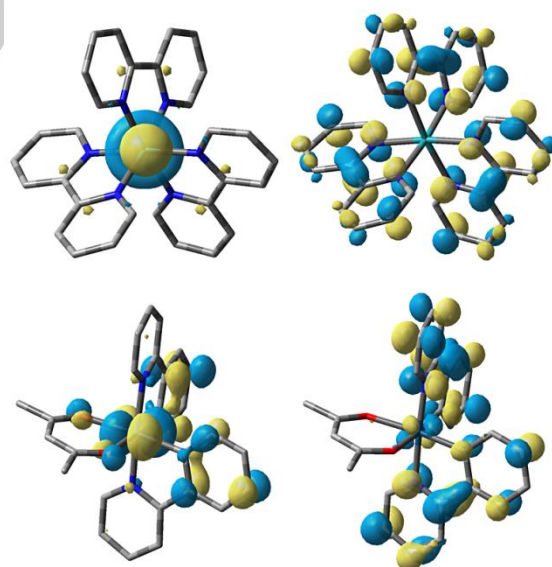
Our potentials for  $\text{Ir}(\text{ppy})_3$  and  $\text{Ir}(\text{ppy})_2(\text{acac})$  were also in good agreement with those reported.<sup>[27]</sup> Our data for  $\text{Ir}(\text{pq})_2(\text{acac})$  and  $[\text{Ru}(\text{bpy})_3]^{2+}$  (Table 2) were within the range of previously reported values, with the exception of the  $E_{ox}^0$  for  $\text{Ir}(\text{pq})_2(\text{acac})$  of 0.46 V vs  $\text{Fc}^{0/+}$ , although this value was similar to the report of Fernandez-Hernandez *et al.* (0.47 V vs  $\text{Fc}^{0/+}$ )<sup>[11]</sup> (Table 1). The

difference in their first reduction and oxidation potentials ( $\Delta E$ ) increased in the order:  $\text{Ir}(\text{ppy})_3 \approx \text{Ir}(\text{ppy})_2(\text{acac}) \ll \text{Ir}(\text{bt})_2(\text{acac}) \ll \text{Ir}(\text{pq})_2(\text{acac}) \approx [\text{Ru}(\text{bpy})_3]^{2+}$  (Tables 1 and 2).

### Theoretical Calculations

The electronic structure and nature of each complex was investigated with DFT calculations. A range of density functionals were considered, including pure and hybrid functionals; in each case the characteristics of the calculated MOs were qualitatively similar and calculated trends were consistent, but the orbital energies (and HOMO-LUMO gaps) were found to be strongly dependent on the proportion of Hartree-Fock exchange in the functional. As a result, only BP86 results (pure exchange-correlation functional without Hartree-Fock exchange) are presented. Having no Hartree-Fock exchange, the calculated HOMO-LUMO gaps represent a lower bound of DFT calculated values. The BP86 results also yield the smallest degree of spin contamination in the oxidized and reduced forms of the complexes (see below).

For the complexes considered here, plots of the frontier MOs are given in Figure 6 and S6. The MOs of  $[\text{Ru}(\text{bpy})_3]^{2+}$  are already well characterised, with a metal-centred HOMO and ligand-based LUMO.<sup>[2e, 29, 32]</sup> The triplet-state spin density (Figure 7 and S7) shares the same spatial extent as the singlet HOMO and LUMO, for which the lowest singlet-triplet transition may be described as metal-to-ligand charge-transfer (MLCT).<sup>[32]</sup> For each of the iridium complexes, there is very little spatial overlap between the singlet-state HOMO and LUMO (*i.e.*, they are largely orthogonal), which indicates that the HOMO and LUMO energies might be independently ‘tuned’ by appropriate substitution of donor/acceptor groups on the ligands.

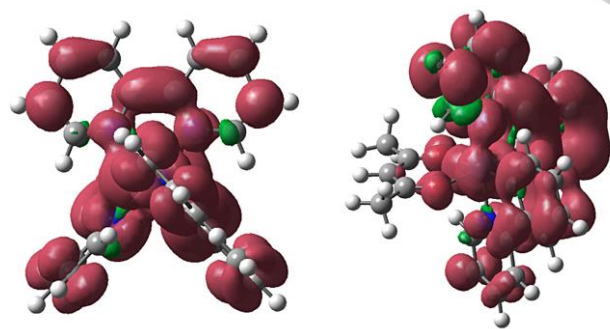


**Figure 6.** BP86/def2-TZVP ground-state singlet MO surfaces of  $[\text{Ru}(\text{bpy})_3]^{2+}$  (top) and  $\text{Ir}(\text{ppy})_2(\text{acac})$  (bottom). The MO plots of all complexes investigated in this study are shown in the ESI (Figure S1).

**Table 2.** Selected spectroscopic, electrochemical and ECL data (obtained in acetonitrile unless otherwise stated).

	Ir(ppy) <sub>3</sub>	Ir(ppy) <sub>2</sub> (acac)	Ir(bt) <sub>2</sub> (acac)	Ir(pq) <sub>2</sub> (acac)	[Ru(bpy) <sub>3</sub> ] <sup>2+</sup>
<b>Luminescence</b>					
PL (r.t.), $\lambda_{\text{max}}/\text{nm}^{[a]}$	520 (516) <sup>[b]</sup>	525 (523)	565, 605 (564, 600)	611 (602)	621 (610)
PL (77 K) $\lambda_{\text{max}}/\text{nm}^{[a],[c]}$	494, 532	501, 537	546, 592, 645	581, 624	580, 628
$E_{0-0}/\text{eV}^{[d]}$	2.51	2.47	2.27	2.13	2.14
ECL, $\lambda_{\text{max}}/\text{nm}^{[a]}$	520	530	567, 602	613	620
<b>Electrochemistry</b>					
$E_{\text{ox}}^0/V$ (vs $\text{Fc}^{0/+}$ )	0.33	0.42	0.58	0.46	0.89
$E_{\text{red}}^0/V$ (vs $\text{Fc}^{0/+}$ )	-2.67	-2.59	-2.24	-2.15	-1.73, -1.92, -2.16
$\Delta E/V$	3.00	3.01	2.82	2.61	2.62
$i_{\text{pa}}/i_{\text{pc}}$ (ox)	1.05	1.06	1.02	1.01	1.02
$i_{\text{pa}}/i_{\text{pc}}$ (red)	1.06	1.04	1.04	0.98	1.07
$E(M^*/M^+)V$ (vs $\text{Fc}^{0/+}$ ) <sup>[e]</sup>	-2.18	-2.05	-1.69	-1.67	-1.25
$E(M^*/M^+)V$ (vs $\text{Fc}^{0/+}$ ) <sup>[f]</sup>	-0.16	-0.12	0.03	-0.02	0.41
<b>Relative ECL Intensity with TPra co-reactant (<math>I_{\text{s}}/I_{\text{ref}}</math>)</b>					
Conditions A	0.016 (0.018) <sup>[b],[g]</sup>	0.033 (0.036)	1.15 (1.19)	3.08 (3.09)	1 <sup>[h]</sup>
Conditions B	<0.001 (0.001)	0.011 (0.012)	0.51 (0.52)	1.13 (1.13)	1
Conditions C	<0.01	2.63 (2.95)	25.1 (26.1)	79.1 (79.5)	1
Conditions D <sup>[i]</sup>	(0.190)	(51.8)	(243.1)	(80.4)	1

<sup>[a]</sup>Luminescence spectra were corrected for the change in instrument sensitivity across the examined wavelength range. The correction factor was established using a light source with standard spectral irradiance. <sup>[b]</sup>Values in parentheses were obtained prior to correction. <sup>[c]</sup>Obtained in 4:1 ethanol:methanol. <sup>[d]</sup>Calculated from PL  $\lambda_{\text{max}}$  at 77 K. <sup>[e]</sup>Calculated:  $E_{\text{ox}}^0 - E_{0-0}$ . <sup>[f]</sup>Calculated:  $E_{\text{red}}^0 + E_{0-0}$ . <sup>[g]</sup>For Conditions A-C, the detection response was fairly uniform across the wavelengths of emission and therefore correction had very little influence on the relative ECL intensities. For Conditions D, the detector response was much poorer towards the red end of the visible spectrum and the ECL intensities were artificially raised (relative to [Ru(bpy)<sub>3</sub>]<sup>2+</sup>), which is more pronounced for the metal complexes with lower wavelengths of emission. <sup>[h]</sup>By definition, the ECL intensity of [Ru(bpy)<sub>3</sub>]<sup>2+</sup> = 1 under each set of conditions. <sup>[i]</sup>Obtained using a PMT as the photodetector instead of the CCD spectrometer.

**Figure 7.** BP86/def2-TZVP calculated triplet spin density surfaces of [Ru(bpy)<sub>3</sub>]<sup>2+</sup> (left) and Ir(ppy)<sub>2</sub>(acac) (right). The triplet spin density surfaces of all complexes investigated in this study are shown in ESI (Figure S2).

Löwdin population analysis of fragment contributions to the HOMO and LUMO is plotted in Figure 8 and S8. Iridium octahedral complexes differ from [Ru(bpy)<sub>3</sub>]<sup>2+</sup> in that the HOMO has a reduced metal d-orbital contribution (typically 50% or less)

compared to that of [Ru(bpy)<sub>3</sub>]<sup>2+</sup> (~80%). The frontier MO characteristics of Ir(ppy)<sub>3</sub> lie between those of the Ir(C<sup>^</sup>N)<sub>2</sub>(acac) complexes and [Ru(bpy)<sub>3</sub>]<sup>2+</sup>, with a greater HOMO metal contribution (58%) than the Ir(C<sup>^</sup>N)<sub>2</sub>(acac) complexes. There are noticeable similarities in the Ir(C<sup>^</sup>N)<sub>2</sub>(acac) compounds: Ir contributes 43-47% of the HOMO while the C<sup>^</sup>N ligand contributes 46-51%. The LUMO is almost exclusively composed of the C<sup>^</sup>N ligand (95%). It is important to note that the LUMO has little density on the acac ligand, which results in the LUMO energies being dependent on the nature of the C<sup>^</sup>N ligand. This observation suggests a simpler strategy of tuning photophysical properties of acac-containing iridium complexes via a straightforward variation of the C<sup>^</sup>N ligand. For example, the energies of the C<sup>^</sup>N centred LUMOs of Ir(ppy)<sub>3</sub> and Ir(ppy)<sub>2</sub>(acac) are very similar (-1.60 and -1.64 eV), but differ from the Ir(pq)<sub>2</sub>(acac) and Ir(bt)<sub>2</sub>(acac) LUMO energies of -2.12 and -1.99 eV, respectively. In contrast, the HOMO energies of each of the Ir(III) complexes are similar (-5.21 to -5.43 eV). The net effect is that the HOMO-LUMO gap is greatest for the Ir(ppy)<sub>3</sub> and Ir(ppy)<sub>2</sub>(acac) complexes, which possess the least stable LUMOs.

For the Ir complexes, the triplet spin density surface (Figure 7 and S7) shares the same spatial extent as the singlet HOMO and LUMO, which in this case leads to a description of the lowest energy excited state as having a mixed MLCT and metal–ligand-to-ligand charge-transfer (MLLCT) character. The trends in HOMO and LUMO energies are in good agreement with the electrochemical results (Figure 9), and the trends in the HOMO–LUMO gaps are consistent with the spectroscopic results (Figure S9), where the energies increase in the order:  $[\text{Ru}(\text{bpy})_3]^{2+} < \text{Ir}(\text{pq})_2(\text{acac}) < \text{Ir}(\text{bt})_2(\text{acac}) < \text{Ir}(\text{ppy})_2(\text{acac}) \leq \text{Ir}(\text{ppy})_3$ .

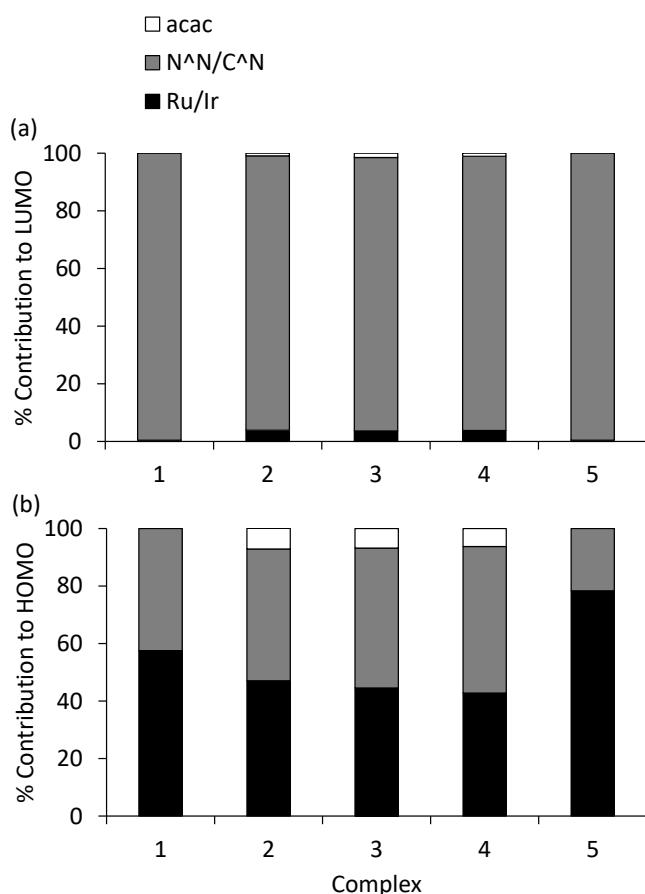


**Figure 8.** Contribution to (a) LUMO and (b) HOMO of metal centre and ligands in: (1)  $\text{Ir}(\text{ppy})_3$ ; (2)  $\text{Ir}(\text{ppy})_2(\text{acac})$ ; (3)  $\text{Ir}(\text{bt})_2(\text{acac})$ ; (4)  $\text{Ir}(\text{pq})_2(\text{acac})$ ; and (5)  $[\text{Ru}(\text{bpy})_3]^{2+}$ . A comparison of the contribution of the Ru/Ir centre to LUMO is shown in ESI (Figure S3).

### Electrogenerated chemiluminescence

We sought to compare the relative ECL intensities of the complexes under oxidative potential with TPrA as co-reactant. Initially, we employed chemical and instrumental conditions (hereafter referred to as 'Conditions A') that were similar to that of our previous comparisons of ECL intensities of various ruthenium and iridium complexes with TPrA co-reactant in acetonitrile.<sup>[2e, 33]</sup> In these previous studies, the electrochemiluminophores were typically compared at a concentration of 0.1 mM with a large excess of the TPrA co-reactant, applying an oxidative overpotential with a glassy carbon working electrode. The ECL intensities were measured by integrating emission spectra

obtained with a spectrometer with a CCD detector. One of the most promising iridium complexes identified in these studies<sup>[2e]</sup> was  $[\text{Ir}(\text{df-ppy})_2(\text{ptb})](\text{PF}_6)$  (where  $\text{df-ppy}$  = 2-(2,4-difluorophenyl)pyridine anion,  $\text{ptb}$  = 1-benzyl-1,2,3-triazol-4-ylpyridine) ( $\text{PL } \lambda_{\text{max}} = 454, 484 \text{ nm}$ ;  $\phi_{\text{PL}} = 0.21$ ), which exhibited a co-reactant ECL intensity that was much greater than a range of other iridium complexes, but still only 0.24 compared to the  $[\text{Ru}(\text{bpy})_3](\text{PF}_6)_2$  reference intensity of 1.

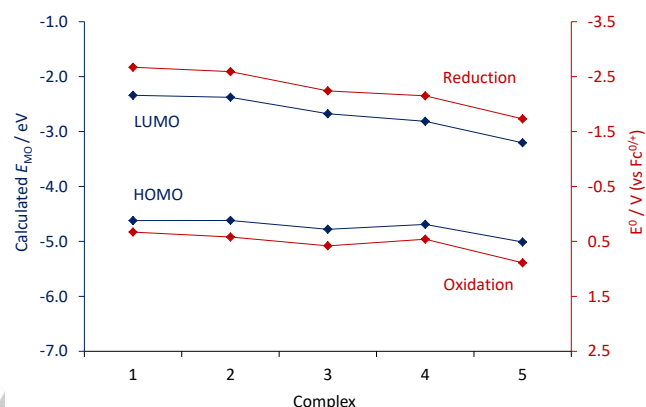


**Figure 9.** Comparison of MO energies (left axis) and electrochemical properties (right axis) of: (1)  $\text{Ir}(\text{ppy})_3$ ; (2)  $\text{Ir}(\text{ppy})_2(\text{acac})$ ; (3)  $\text{Ir}(\text{bt})_2(\text{acac})$ ; (4)  $\text{Ir}(\text{pq})_2(\text{acac})$ ; and (5)  $[\text{Ru}(\text{bpy})_3]^{2+}$ .

Under Conditions A, the co-reactant ECL intensities of  $\text{Ir}(\text{bt})_2(\text{acac})$  and  $\text{Ir}(\text{pq})_2(\text{acac})$  were 1.19 and 3.09 relative to the  $[\text{Ru}(\text{bpy})_3](\text{PF}_6)_2$  reference, which exceeded that of the previously reported  $[\text{Ir}(\text{df-ppy})_2(\text{ptb})](\text{PF}_6)$  complex (nb: the additional  $I_{\text{s}}/I_{\text{ref}}$  values shown in parentheses in Table 2 were obtained without correction for the sensitivity of the instrumentation across the wavelength range; the similarity with those obtained after correction show the reasonable consistency of the CCD spectrometer response across the investigated range). However, these values were well below the reported 214 for  $\text{Ir}(\text{bt})_2(\text{acac})$ ,<sup>[10]</sup> and either  $10^{[9]}$  or  $77^{[2a]}$  for  $\text{Ir}(\text{pq})_2(\text{acac})$  (Table 1). The relative ECL intensity for  $\text{Ir}(\text{ppy})_2(\text{acac})$  (0.036) was also more than an order of magnitude lower than that previously reported (0.96).<sup>[10]</sup> In an attempt to understand the large discrepancies between the observed and reported values, we considered numerous factors that could influence these ratios:

(1) **Decomposition.** The  $\text{Ir}(\text{C}^{\wedge}\text{N})_2(\text{acac})$  complexes can decompose by exchange of the acac ligand with solvent molecules.<sup>[34]</sup> However, the presence of acid is required for this to occur at an appreciable rate, and none of the characteristic changes in the absorption or emission spectra associated with this decomposition<sup>[34]</sup> were observed under the chemical conditions used in this study.

(2) **Solvent.** Bruce and Richter reported co-reactant ECL efficiencies for  $\text{Ir}(\text{ppy})_3$  of 0.33 in ACN, 0.0044 in mixed ACN and aqueous solution (1:1 v/v) and 0.00092 in aqueous solution (relative to  $[\text{Ru}(\text{bpy})_3]^{2+} = 1$ ).<sup>[3a]</sup> In contrast, Xia *et al.* recently reported increases in the co-reactant ECL of  $\text{Ir}(\text{bt})_2(\text{acac})$ ,  $\text{Ir}(\text{pq})_2(\text{sa})$  and  $\text{Ir}(\text{pq})_2(\text{psa})$  (where sa = succinylacetone; psa = 4,6-dioxo-6-phenylhexanoic acid) with TPrA in air-saturated ACN upon the addition of water, which was attributed to keto-enol

tautomerism of the ancillary ligand.<sup>[35]</sup> It is therefore likely that even traces of water in the solvent will affect the relative ECL intensity for  $\text{Ir}(\text{ppy})_3$  and  $\text{Ir}(\text{C}^{\wedge}\text{N})_2(\text{acac})$  complexes. In our study, the ACN was freshly distilled over calcium hydride under nitrogen and we are confident that it would be at least as dry as that used in the previous reports of relative ECL intensities. In one of the previous studies,<sup>[10]</sup> Zhou *et al.* compared the ECL intensities of the  $\text{Ir}(\text{ppy})_2(\text{acac})$  and  $\text{Ir}(\text{bt})_2(\text{acac})$  complexes in dichloromethane (DCM) rather than ACN. Although both are organic, aprotic solvents, they provide a different electrochemical potential window, and Zhou *et al.* could not measure the reduction peaks of the complexes in DCM.<sup>[10]</sup> The potential window can affect the stability of certain reactive intermediates of the multiple possible ECL reaction pathways.<sup>[8]</sup> This is elaborated in item 5 below.

(3) *Deaeration.* The longer excited-state lifetimes of the iridium(III) complexes than  $[\text{Ru}(\text{bpy})_3]^{2+}$  (Table 1) make them more susceptible to quenching by dissolved molecular oxygen, thus reducing their relative ECL intensity in its presence. With our experimental approach, which includes purging each solution in the electrochemical cell with argon for 15 min, we do not believe that the presence of any remaining oxygen was responsible for the much lower relative ECL intensities found under these conditions than those previously reported.<sup>[2a, 3a, 9-10]</sup> Moreover, the presence of oxygen is easily seen by cyclic voltammetry, and was not observed in our experiments.

(4) *Electrode materials and applied potentials.* The instrumental conditions for the evaluation of relative co-reactant ECL intensities are not standardised, and a survey of the literature shows a variety of different electrode materials and applied potentials that include the use of a single voltage for a set of complexes (e.g., 1.2 V<sup>[9]</sup> or 1.4 V vs  $\text{Fc}^{0/+}$ <sup>[2e, 33b]</sup>) and various voltages beyond the  $E_{\text{ox}}$  of each complex under investigation (e.g., 0.08 V,<sup>[10]</sup> 0.1 V,<sup>[36]</sup> or 0.5 V<sup>[2a]</sup>). In their study in which they reported a relative co-reactant ECL intensity of 77 for  $\text{Ir}(\text{pq})_2(\text{acac})$ , Kim *et al.*<sup>[2a]</sup> used the same reactant and electrolyte concentrations as our *Conditions A*, but they used a platinum disk working electrode and a higher overpotential ( $E_{\text{ox}} + 0.5$  V), which was applied at 10 Hz for 10 s (total of 100 pulses). We attempted to replicate these experimental parameters (*Conditions B*), but observed a further decrease in the relative co-reactant ECL intensities of the iridium complexes compared to  $[\text{Ru}(\text{bpy})_3]^{2+}$  (Table 2). However, during these experiments it became evident that the decrease in ECL intensity with each subsequent applied potential pulse (of a single experiment) was less prominent for the  $\text{Ir}(\text{C}^{\wedge}\text{N})_2(\text{acac})$  complexes than for  $[\text{Ru}(\text{bpy})_3]^{2+}$ . Therefore, an increase in the number of pulses produced an increase in the ECL intensities of the  $\text{Ir}(\text{C}^{\wedge}\text{N})_2(\text{acac})$  complexes relative to that of  $[\text{Ru}(\text{bpy})_3]^{2+}$ , because the ECL intensity is integrated over the time period of the experiment (all pulses).

(5) *Reactant concentration.* The mechanism of co-reactant ECL with TPrA comprises several reaction pathways to the electronically excited state species that is responsible for the emission of light.<sup>[8]</sup> TPrA can be oxidised at the electrode (Eqn 2) or by the oxidised metal complex (Eqn 3) to form the corresponding aminium radical cation, denoted  $\text{TPrA}^{+\bullet}$ , which rapidly deprotonates to generate a highly reductive neutral  $\alpha$ -amino alkyl radical, denoted  $\text{TPrA}^{\bullet}$  (Eqn 4). The emitting

species can then be generated by direct reaction between the oxidised metal complex and  $\text{TPrA}^{\bullet}$  (Eqn 5), or via reduction of the metal complex by  $\text{TPrA}^{\bullet}$  (Eqn 6), followed by annihilation of the oxidised and reduced metal complex (Eqn 7), or reaction of the reduced metal complex with  $\text{TPrA}^{+\bullet}$  (Eqn 8). When comparing the potentials of the Ir complexes under investigation with those of TPrA (for which a peak potential was obtained at 0.43 V vs  $\text{Fc}^{0/+}$  using square wave voltammetry<sup>[15]</sup>) and  $\text{TPrA}^{\bullet}$  (estimated at -2.1 V vs  $\text{Fc}^{0/+}$ <sup>[37]</sup>), we find that Eqn 1-9 are not all energetically feasible for the Ir(III) complexes. Kim *et al.* attributed the intense ECL for  $\text{Ir}(\text{pq})_2(\text{acac})$  with TPrA in acetonitrile in part to an efficient transfer of electrons in Eqn 3 and 6,<sup>[2a]</sup> but Eqn 3 is not feasible for  $\text{Ir}(\text{ppy})_2(\text{acac})$  and  $\text{Ir}(\text{ppy})_3$ , and Eqn 6 (and therefore also Eqn 7 and 8) is not feasible for  $\text{Ir}(\text{bt})_2(\text{acac})$ ,  $\text{Ir}(\text{ppy})_2(\text{acac})$  and  $\text{Ir}(\text{ppy})_3$ . This, however, does not rule out the generation of ECL for these complexes, which can still occur via Eqns 1, 2, 4, 5 and 9.

For each feasible reaction pathway, the intensity of the ECL at any particular moment will be dependent on the rate that the emitting species is generated, which is dependent in part on the concentration of the reactants required for each step. The initial concentration of the metal complex and the co-reactant, and any experimental condition that influences the formation or stability of the intermediates, will influence the rate and relative contribution of the reaction pathways. This may include the electrode materials and geometry, the cell configuration and dimensions, the solvent and electrolyte, and the magnitude and sequence of the applied potentials. For example, Zhou *et al.*<sup>[9]</sup> found that the co-reactant ECL intensity of  $\text{Ir}(\text{pq})_2(\text{acac})$  (relative to  $[\text{Ru}(\text{bpy})_3]^{2+} = 1$ ) was 10.3 when the applied potential was stepped to 1.2 V (vs  $\text{Fc}^{0/+}$ ), but increased to 42.5 when the potential was instead scanned at 0.1 V s<sup>-1</sup> from 0.4 V to 1.2 V, which would have generated different concentrations of the key intermediates of the reaction pathways. Although many of the above parameters are difficult to examine, we can manipulate the rate and contribution of the distinct reaction pathways by changing the concentrations of the two starting reactants (the metal complex and the co-reactant), which achieves similar outcomes in terms of the relative ECL intensities.

Decreasing the concentration of the metal complex by two orders of magnitude (whilst also increasing the number of applied potential pulses to compensate for the reduced intensity) produced an increase in the relative intensity for  $\text{Ir}(\text{bt})_2(\text{acac})$ , but a decrease for the other iridium complexes. In contrast, decreasing the concentration of TPrA instead by two orders of magnitude gave a large increase for each  $\text{Ir}(\text{C}^{\wedge}\text{N})_2(\text{acac})$  complex relative to that of  $[\text{Ru}(\text{bpy})_3]^{2+}$ . Surprisingly, an even greater increase in the relative intensities of the  $\text{Ir}(\text{C}^{\wedge}\text{N})_2(\text{acac})$  complexes was observed when decreasing the concentrations of both starting reactants (*Conditions C* in Table 2). Under these conditions, the relative intensity for  $\text{Ir}(\text{pq})_2(\text{acac})$  ( $I_{\text{S}}/I_{\text{ref}} = 81.9$ ) was now well above that reported by Zhou *et al.* ( $I_{\text{S}}/I_{\text{ref}} = 10$ ) and similar to that reported by Kim *et al.* ( $I_{\text{S}}/I_{\text{ref}} = 77$ ).<sup>[2a]</sup> The intensities for  $\text{Ir}(\text{bt})_2(\text{acac})$  ( $I_{\text{S}}/I_{\text{ref}} = 26.8$ ) and  $\text{Ir}(\text{ppy})_2(\text{acac})$  ( $I_{\text{S}}/I_{\text{ref}} = 0.50$ ) were also greatly increased compared to those obtained using *Conditions A*, but still below those reported by Zhou *et al.*<sup>[10]</sup> ( $I_{\text{S}}/I_{\text{ref}} = 214$  and 0.96, respectively; Table 1). It should be noted that the concentrations of metal complex and TPrA used in the comparisons of ECL intensities by Kim *et al.*<sup>[2a]</sup> and Zhou *et al.*<sup>[9]</sup>



<sup>10]</sup> were the same or similar to those that we used in *Conditions A* and *B*, and that we only utilised these lower concentrations here as a means to manipulate the generation of key reaction intermediates to represent the possible effects of a range of other parameters as described above.

(6) *Spectral sensitivity*. For complexes that have a similar spectral distribution, such as the orange-red light emitters: Ir(pq)<sub>2</sub>(acac) and [Ru(bpy)<sub>3</sub>]<sup>2+</sup> (Figure 3), changes in the sensitivity of the photodetector over the wavelength range will have only minor effects on the relative intensity of the two complexes. In their evaluation of the Ir(pq)<sub>2</sub>(acac) complex, Kim *et al.*<sup>[2a]</sup> obtained spectra with a Princeton Instruments charge-coupled device (CCD) camera and used the integrated area of the spectrum, whereas Zhou *et al.*<sup>[9]</sup> used an unspecified PMT and integrated the signal over time. Although it could be expected that the CCD-based approach would provide a more consistent response over the wavelengths of the emission bands, this would be unlikely to explain the difference in their reported relative ECL intensities ( $I_s/I_{ref}$  of 77 and 10, respectively), due to the similarity of the emission wavelengths of the evaluated and reference complexes.

However, the other three iridium complexes (which emit yellow or green light; Figure 3) have a very different spectral distribution to that of [Ru(bpy)<sub>3</sub>]<sup>2+</sup>, and photodetectors that have much lower sensitivity in the red region of the spectrum (such as typical photomultiplier tubes) will give artificially high ECL intensities for these complexes relative to the [Ru(bpy)<sub>3</sub>]<sup>2+</sup> reference. In their evaluation of the Ir(bt)<sub>2</sub>(acac) and Ir(ppy)<sub>2</sub>(acac) complexes, Zhou *et al.*<sup>[10]</sup> used a MPI-A detector (Xi'an Remax Electronics, China) for ECL measurement, and a Cary Eclipse fluorescence spectrophotometer to collect ECL spectra (without spectral correction). It is unclear which of these instruments was used to obtain the relative ECL intensities, but both contain a photomultiplier tube that will significantly less sensitive to the longer wavelengths of the reference complex. In the evaluation of Ir(ppy)<sub>3</sub> by Bruce *et al.*<sup>[3a]</sup> they refer to previous papers for the details of the instrumentation, which include a photomultiplier tube (Hamamatsu HC 135) for the measurement of ECL,<sup>[38]</sup> and a Shimadzu RF-5301 spectrofluorophotometer (without spectral correction) for ECL spectra.<sup>[38b]</sup> They do state, however, that the ECL efficiencies were obtained by the literature methods using [Ru(bpy)<sub>3</sub>]<sup>2+</sup> ( $\phi_{ECL} = 1$ ) as the standard, and cite a paper in which a charge-coupled device (CCD) camera system was employed,<sup>[39]</sup> but it is unclear which instrumentation was utilised for the evaluation of Ir(ppy)<sub>3</sub>.

For our *Conditions A-C*, we used an Ocean Optics spectrometer that exhibits a much flatter spectral response of the region of interest than a PMT. This is seen in the similar  $\lambda_{max}$  of the ECL spectra collected with the CCD spectrometer using an emission slit that provided a 6.5 nm resolution, with the respective photoluminescence spectra obtained with a Cary Eclipse with an emission bandpass of 5 nm, but only after correction of the photoluminescence spectra for the relative spectral sensitivity of the Eclipse (Table 2). The artificial hypsochromic shift of the uncorrected photoluminescence emission spectra (particularly Ir(pq)<sub>2</sub>(acac) and [Ru(bpy)<sub>3</sub>]<sup>2+</sup>) results from the poorer sensitivity of the instrument in the red end of the visible range. The Eclipse

contains an extended-range multi-alkali PMT (model R928; Hamamatsu), whereas typical bialkali PMTs are even less sensitive in that region.

*Conditions D* were a repeat of *Conditions C*, except that we replaced the CCD spectrometer with a bialkali PMT (and the acquisition time was reduced). The relative ECL intensity of Ir(pq)<sub>2</sub>(acac) was similar, due to the similarity of its spectrum with that of the reference complex (Figure 3). However, the other three complexes emit light at shorter wavelengths, where the PMT is considerably more sensitive, resulting in an artificial increase in their measured ECL intensities relative to the [Ru(bpy)<sub>3</sub>]<sup>2+</sup>. Under these conditions, our  $I_s/I_{ref}$  value for Ir(bt)<sub>2</sub>(acac) was similar to that reported by Zhou *et al.*,<sup>[10]</sup> but our  $I_s/I_{ref}$  for Ir(ppy)<sub>2</sub>(acac) was far beyond that reported by Zhou *et al.* in the same study.

## Conclusions

The evaluation of ECL  $I_s/I_{ref}$  is vulnerable to influence from a range of experimental parameters and in some cases, exceptional intensities reported for new complexes may have been derived using instrumental or chemical conditions that unintentionally disadvantaged the [Ru(bpy)<sub>3</sub>]<sup>2+</sup> reference electrochemiluminophore, such as the electrochemical pulse sequence or the use of photodetectors that are less sensitive towards the red end of the spectrum where the reference complex emits light. However, although the wavelength sensitivity of typical photomultiplier tubes may bias the relative ECL intensities towards electrochemiluminophores that emit light near the blue-end of the spectrum, this comparison may be more practical if the final analytical instrumentation for which the detection system is used exhibits a similar bias. The light-producing reaction pathways identified for the classic [Ru(bpy)<sub>3</sub>]<sup>2+</sup>-TPrA co-reactant ECL system are not necessarily all feasible for novel electrochemiluminophores, which is an important consideration for the intended application. For example, in ECL-based immunodiagnostic systems in which the metal-complex labels are immobilised on magnetic microbeads held at an electrode surface, generation of ECL relies predominantly on the diffusion of oxidised TPrA radicals from the electrode to the bound electrochemiluminophores (*i.e.*, Eqn 2, 4, 6 and 8).<sup>[8]</sup> Eqn 6 and 8 are not feasible for most of the iridium complexes examined in this study. Conversely, in systems in which the metal complex is used for the ECL detection of an amine analyte,<sup>[1b, 40]</sup> both species can be oxidised at the electrode surface and pathways analogous to Eqns 1-5 become more important. When comparing relative ECL intensities, it is therefore also important to consider the influence of experimental conditions on the relative contribution of multiple reaction pathways that may be available for complexes within the study.

## Experimental Section

**Chemicals.** [Ru(bpy)<sub>3</sub>](PF<sub>6</sub>)<sub>2</sub>, Ir(ppy)<sub>3</sub> and tetrabutylammonium hexafluorophosphate (TBAPF<sub>6</sub>) were purchased from Sigma-Aldrich (NSW, Australia). Ir(ppy)<sub>2</sub>(acac), Ir(bt)<sub>2</sub>(acac) and Ir(pq)<sub>2</sub>(acac) were

purchased from SunaTech (Jiangsu, China). Acetonitrile was from Scharlau (Barcelona, Spain) and was distilled over calcium hydride under nitrogen. Bis(cyclopentadienyl)iron (ferrocene) was purchased from Strem Chemicals (MA, USA).

**Absorption and photoluminescence emission spectra.** Absorption spectra were obtained using 1 cm pathlength quartz cells with a Cary 300 Bio UV/Vis spectrophotometer (Varian Australia, Vic., Australia). Photoluminescence spectra were collected using a 1 cm quartz cuvette with a Cary Eclipse spectrofluorimeter (Varian Australia; 5 nm band pass, 1 nm data interval, PMT voltage: 800 V). Low temperature (77 K) photoluminescence were obtained using an OptistatDN Variable Temperature Liquid Nitrogen Cryostat, with custom-made quartz sample holder. Room temperature and low temperature emission spectra were corrected for the change in instrument sensitivity across the wavelength range under examination, using a correction factor that was established using a quartz-halogen tungsten lamp of standard spectral irradiance (OL 245M, Optronic Laboratories, FL, USA), operated at 6.5A dc from a programmable current source (OL 65A, Optronic Laboratories).

**Electrochemistry and ECL.** Cyclic voltammetry experiments were performed using an Autolab PGSTAT204 potentiostat (Metrohm Autolab B.V., Netherlands). The electrochemical cell consisted of a cylindrical glass cell with a quartz base and Teflon cover with spill tray.<sup>[41]</sup> The cell and accessories were encased in a custom-built light-tight faraday cage. A conventional three-electrode configuration was employed, consisting of a glassy carbon (3 mm diameter) working electrode shrouded in Teflon (CH Instruments, Austin, TX, USA), silver wire reference electrode and platinum wire counter electrode. The metal complexes were prepared at a concentration of 0.25 mM (with 0.1 M TBAPF<sub>6</sub> as the supporting electrolyte) in freshly distilled acetonitrile. Prior to each experiment, the working electrode was polished using 0.3 mm and then 0.05 mm alumina with water on a felt pad, sonicated in MilliQ water (1 min), rinsed in freshly distilled acetonitrile and dried with a stream of N<sub>2</sub>. The solutions were degassed within the electrochemical cell for 15 min. CVs were collected at a scan rate of 0.1 V s<sup>-1</sup>. Electrochemical potentials were referenced to the ferrocene/ferrocenium (Fc<sup>0/+</sup>) couple measured *in situ* (1 mM) at the end of each experiment. ECL experiments were performed with an Autolab PGSTAT128N potentiostat. The light was detected using an Ocean Optics QE65Pro spectrometer with HC-1 (300 l/mm) grating and Hamamatsu S7031-1006 back-thinned CCD (Quark Photonics, Vic., Australia) via optical fibre (1.0 m length, 1.0 mm core diameter) and collimating lens (Ocean Optics 74-UV, 200-2000 nm), positioned under the transparent base of the electrochemical cell described above, and vertically aligned with the face of the working electrode that was 2 mm above the base of the cell. The spectrometer was fitted with a 200 µm entrance slit, which provided a spectral resolution of 6.5 nm (FWHM). Acquisition was triggered using a HR 4000 Break-Out box in conjunction with the potentiostat. The spectra were corrected for the change in instrument sensitivity across the wavelength range (including absorption from the optical fibre and the lens, features in the grating response and the CCD detector response) using correction factors (one for each slit width setting) that were established using an HL-2000 Ocean Optics light source directed onto a WS-1-SL diffuse white reflectance standard. The spectra were integrated to determine the relative ECL intensities. Prior to each experiment, solutions were purged with grade 5 argon within the electrochemical cell for 15 min.

**ECL Conditions A:** Electrodes: glassy carbon working (3 mm diameter), Ag/AgCl low-leakage reference (Innovative Instruments, FL, USA), and platinum counter. Concentrations: 0.1 mM metal complex, 10 mM TPA, and 0.1 M TBAPF<sub>6</sub> supporting electrolyte. Applied potential: {E<sub>ox</sub> + 0.15 V} for 0.05 s at 10 Hz, 2 s acquisition time (total of 20 pulses). The entrance slit of the spectrometer was removed and replaced with a round SMA with

no slit installed, to increase the proportion of light reaching the CCD detector, resulting in an effective spectral resolution of 30 nm (FWHM).

**ECL Conditions B:** Electrodes: platinum working (2 mm diameter), silver wire reference, and platinum counter. Concentrations: 0.1 mM complex, 10 mM TPA, and 0.1 M TBAPF<sub>6</sub>. Applied potential: {E<sub>ox</sub> + 0.50 V} for 0.05 s at 10 Hz, 10 s acquisition time (100 pulses). The spectrometer was fitted with a 200 µm entrance slit.

**ECL Conditions C:** Electrodes: glassy carbon working (3 mm diameter), Ag/AgCl low-leakage reference, and platinum counter. Concentrations: 0.001 mM complex, 0.1 mM TPA, and 0.1 M TBAPF<sub>6</sub>. Applied potential: {E<sub>ox</sub> + 0.15 V} for 0.05 s at 10 Hz, 30 s acquisition time (300 pulses). The entrance slit of the spectrometer was removed and replaced with a round SMA as described above.

**ECL Conditions D:** Electrodes: glassy carbon working (3 mm diameter), Ag/AgCl low-leakage reference, and platinum counter. Concentrations: 0.001 mM complex, 0.1 mM TPA, and 0.1 M TBAPF<sub>6</sub>. Applied potential: {E<sub>ox</sub> + 0.15 V} for 0.05 s at 10 Hz, 1 s acquisition time (10 pulses). The CCD spectrometer and fibre optic assembly were replaced with a bi-alkali photomultiplier tube (ET Enterprises model 9125SB; ETP, NSW, Australia), positioned directly under the transparent base of the electrochemical cell. The PMT was set at a constant voltage of 800 V from a stable power supply (PM20D, ETP) via a voltage divider (E637-09, ETP). The output from the PMT was connected to the auxiliary channel of the potentiostat via an amplifier (A1, ETP).

**Computational methods.** DFT calculations were carried out within the Gaussian 09 suite of programs.<sup>[42]</sup> Ground and triplet state geometries were optimised in the absence of solvent with the mPW1PW91 functional<sup>[43]</sup> in conjunction with the def2-SVP basis set and associated effective core potential.<sup>[44]</sup> The mPW1PW91 functional has previously been demonstrated to yield reliable results for such systems.<sup>[29, 33b, 45]</sup> Stationary points were characterised as minima by calculating the Hessian matrix analytically at the same level of theory. All structures are minima with no imaginary frequencies. Due to difficulties with the D<sub>3</sub> symmetry triplet state of [Ru(bpy)<sub>3</sub>]<sup>2+</sup>, a previously reported<sup>[46]</sup> B3PW91/LANL2DZ calculated structure was used. Single-point energy calculations (including molecular orbital (MO) energies) were carried out with the def2-TZVP basis set and core potential<sup>[44]</sup> together with DFT functionals with varying amounts of Hartree-Fock exchange: pure functionals PBE,<sup>[47]</sup> and BP86,<sup>[48]</sup> the hybrid functionals PBE0,<sup>[49]</sup> B3LYP,<sup>[50]</sup> and mPW1PW91,<sup>[43]</sup> and long range corrected functionals CAM-B3LYP,<sup>[51]</sup> and B97XD.<sup>[52]</sup> Solvent effects were included for all single-point energy calculations with acetonitrile for consistency with the experimental system. The polarisable continuum model (PCM)<sup>[53]</sup> self-consistent reaction field (SCRF) was used together with Truhlar's SMD solvent model.<sup>[54]</sup> TD-DFT calculations of absorption and emission were calculated at the CAM-B3LYP/def2-SVP level of theory. Absorbance bands were calculated at the singlet-state optimised geometry; 20 singlet and triplet states were calculated with TD-DFT. An SCF convergence criterion of 10<sup>-8</sup> a.u. was employed throughout. MO analysis was carried out with the QMForge program.<sup>[55]</sup>

## Acknowledgements

This work was funded by the Australian Research Council (DP160103046), and the Collaborative 'Cross-SRCs' Funding Scheme of the School of Life and Environmental Sciences, Deakin University. We thank Stuart Rumble (Quark Photonics, Australia) for his assistance in creating the correction factor for

[1] a) M. M. Richter, *Chem. Rev.* **2004**, *104*, 3003-3036; b) A. Gorman, P. S. Francis, N. W. Barnett, *Analyst* **2006**, *131*, 616-639; c) W. Miao, *Chem. Rev.* **2008**, *108*, 2506-2553; d) L. Hu, G. Xu, *Chem. Soc. Rev.* **2010**, *39*, 3275-3304; e) Y. Yuan, S. Han, L. Hu, S. Parveen, G. Xu, *Electrochim. Acta* **2012**, *82*, 484-492; f) X. Zhou, D. Zhu, Y. Liao, W. Liu, Z. Ma, D. Xing, *Nat. Protoc.* **2014**, *9*, 1146-1159; g) K. Muzyka, *Biosens. Bioelectron.* **2014**, *54*, 393-407; h) Z. Liu, W. Qi, G. Xu, *Chem. Soc. Rev.* **2015**, *44*, 3117-3142; i) M. Hesari, Z. Ding, *J. Electrochem. Soc.* **2016**, *163*, H3116-H3131.

[2] a) J. I. Kim, I.-S. Shin, H. Kim, J.-K. Lee, *J. Am. Chem. Soc.* **2005**, *127*, 1614-1615; b) S. Zananini, E. Rampazzo, S. Bonacchi, R. Juris, M. Marcaccio, M. Montalti, F. Paolucci, L. Prodi, *J. Am. Chem. Soc.* **2009**, *131*, 14208-14209; c) S. Zananini, M. Felici, G. Valentini, M. Marcaccio, L. Prodi, S. Bonacchi, P. Contreras-Carballada, R. M. Williams, M. C. Feiters, R. J. M. Nolte, L. De Cola, F. Paolucci, *Chem. Eur. J.* **2011**, *17*, 4640-4647; d) K. N. Swanick, S. Ladouceur, E. Zysman-Colman, Z. Ding, *Chem. Commun.* **2012**, *48*, 3179-3181; e) G. J. Barbante, E. H. Doeven, E. Kerr, T. U. Connell, P. S. Donnelly, J. M. White, T. López, S. Laird, C. F. Hogan, D. J. D. Wilson, P. J. Barnard, P. S. Francis, *Chem. Eur. J.* **2014**, *20*, 3322-3332; f) A. Kapturkiewicz, *Anal. Bioanal. Chem.* **2016**, In press. DOI 10.1007/s00216-016-9615-8.

[3] a) D. Bruce, M. M. Richter, *Anal. Chem.* **2002**, *74*, 1340-1342; b) B. D. Muegge, M. M. Richter, *Anal. Chem.* **2004**, *76*, 73-77; c) E. H. Doeven, E. M. Zammit, G. J. Barbante, C. F. Hogan, N. W. Barnett, P. S. Francis, *Angew. Chem., Int. Ed.* **2012**, *51*, 4354-4357; d) E. H. Doeven, G. J. Barbante, E. Kerr, C. F. Hogan, J. A. Endler, P. S. Francis, *Anal. Chem.* **2014**, *86*, 2727-2732; e) E. H. Doeven, G. J. Barbante, C. F. Hogan, P. S. Francis, *ChemPlusChem* **2015**, *80*, 456-470.

[4] a) K. Nishimura, Y. Hamada, T. Tsujioka, K. Shibata, T. Fuyuki, *Jpn. J. Appl. Phys., Part 2* **2001**, *40*, L945-L947; b) E. M. Gross, N. R. Armstrong, R. M. Wightman, *J. Electrochem. Soc.* **2002**, *149*, E137-E142; c) A. Kapturkiewicz, G. Angulo, *Dalton Trans.* **2003**, 3907-3913.

[5] a) A. Kapturkiewicz, T.-M. Chen, I. R. Laskar, J. Nowacki, *Electrochem. Commun.* **2004**, *6*, 827-831; b) A. Kapturkiewicz, J. Nowacki, P. Borowicz, *Electrochim. Acta* **2005**, *50*, 3395-3400.

[6] a) S. Lamansky, P. Djurovich, D. Murphy, F. Abdel-Razzaq, H.-E. Lee, C. Adachi, P. E. Burrows, S. R. Forrest, M. E. Thompson, *J. Am. Chem. Soc.* **2001**, *123*, 4304-4312; b) B. W. D'Andrade, M. E. Thompson, S. R. Forrest, *Adv. Mater.* **2002**, *14*, 147-151; c) D. Kolosov, V. Adamovich, P. E. H. Doeven, E. M. Zammit, G. J. Barbante, P. S. Francis, N. W. Barnett, C. F. Hogan, *Chem. Sci.* **2013**, *4*, 977-982.

[16] K. Dedeian, P. I. Djurovich, F. O. Garces, G. Carlson, R. J. Watts, *Inorg. Chem.* **1991**, *30*, 1685-1687.

[17] K. Nakamaru, *J. Chem. Soc. Jpn.* **1982**, *55*, 2697-2705.

[18] P. I. Djurovich, D. Murphy, M. E. Thompson, B. Hernandez, R. Gao, P. L. Hunt, M. Selke, *Dalton Trans.* **2007**, 3763-3770.

[19] A. Tsuboyama, H. Iwawaki, M. Furugori, T. Mukaide, J. Kamatani, S. Igawa, T. Moriyama, S. Miura, T. Takiguchi, S. Okada, M. Hoshino, K. Ueno, *J. Am. Chem. Soc.* **2003**, *125*, 12971-12979.

[20] B. Beyer, C. Ulbricht, D. Escudero, C. Friebe, A. Winter, L. Gonzalez, U. S. Schubert, *Organometallics* **2009**, *28*, 5478-5488.

[21] Q. Zhao, C.-Y. Jiang, M. Shi, F.-Y. Li, T. Yi, Y. Cao, C.-H. Huang, *Organometallics* **2006**, *25*, 3631-3638.

[22] A. Juris, V. Balzani, P. Belser, A. von Zelewsky, *Helv. Chim. Acta* **1981**, *64*, 2175-2182.

[23] A. Endo, K. Suzuki, T. Yoshihara, S. Tobita, M. Yahiro, C. Adachi, *Chem. Phys. Lett.* **2008**, *460*, 155-157.

[24] T. Hofbeck, H. Yersin, *Inorg. Chem.* **2010**, *49*, 9290-9299.

[25] T. Sajoto, P. I. Djurovich, A. B. Tamayo, J. Oxgaard, W. A. Goddard, M. E. Thompson, *J. Am. Chem. Soc.* **2009**, *131*, 9813-9822.

[26] K. A. King, P. J. Spellane, R. J. Watts, *J. Am. Chem. Soc.* **1985**, *107*, 1431-1432.

[27] F.-C. Chen, S.-C. Chang, G. He, S. Pyo, Y. Yang, M. Kurotaki, J. Kido, *J. Polym. Sci., Part B: Polym. Phys.* **2003**, *41*, 2681-2690.

[28] I.-S. Shin, J. I. Kim, T.-H. Kwon, J.-I. Hong, J.-K. Lee, H. Kim, *J. Phys. Chem. C* **2007**, *111*, 2280-2286.

[29] G. J. Barbante, C. F. Hogan, D. J. D. Wilson, N. A. Lewcenko, F. M. Pfeffer, N. W. Barnett, P. S. Francis, *Analyst* **2011**, *136*, 1329-1338.

[30] N. E. Tokel-Takvoryan, R. E. Hemingway, A. J. Bard, *J. Am. Chem. Soc.* **1973**, *95*, 6582-6589.

[31] P. Szrebrowaty, A. Kapturkiewicz, *Chem. Phys. Lett.* **2000**, *328*, 160-168.

[32] S. Campagna, F. Puntoriero, F. Nastasi, G. Bergamini, V. Balzani, *Top. Curr. Chem.* **2007**, *280*, 117-214.

[33] a) T. Joshi, G. J. Barbante, P. S. Francis, C. F. Hogan, A. M. Bond, G. Gasser, L. Spiccia, *Inorg. Chem.* **2012**, *51*, 3302-3315; b) G. J. Barbante, E. H. Doeven, P. S. Francis, B. D. Stringer, C. F. Hogan, P. R. Kheradmand, D. J. D. Wilson, P. J. Barnard, *Dalton Trans.* **2015**, *44*, 8564-8576.

[34] Y. Li, Y. Liu, M. Zhou, *Dalton Trans.* **2012**, *41*, 3807-3816.

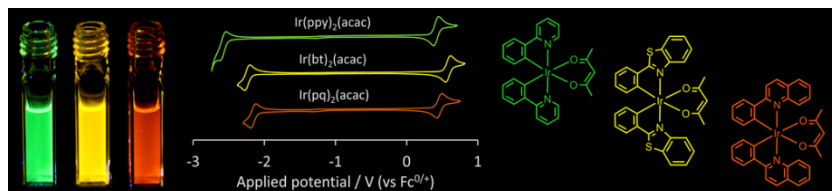


- [35] S. Xia, D. Han, H. Gao, Y. Zhao, H. Qi, C. Zhang, *J. Electroanal. Chem.* **2016**, *777*, 101-107.
- [36] a) B. D. Stringer, L. M. Quan, P. J. Barnard, D. J. D. Wilson, C. F. Hogan, *Organometallics* **2014**, *33*, 4860-4872; b) E. Kerr, E. H. Doeven, G. J. Barbante, T. U. Connell, P. S. Donnelly, D. J. D. Wilson, T. D. Ashton, F. M. Pfeffer, P. S. Francis, *Chem. - Eur. J.* **2015**, *21*, 14987-14995.
- [37] R. Y. Lai, A. J. Bard, *J. Phys. Chem. A* **2003**, *107*, 3335-3340.
- [38] a) J. McCall, C. Alexander, M. M. Richter, *Anal. Chem.* **1999**, *71*, 2523-2527; b) S. R. Workman, Mark M., *Anal. Chem.* **2000**, *72*, 5556-5561.
- [39] P. McCord, A. J. Bard, *J. Electroanal. Chem. Interfacial Electrochem.* **1991**, *318*, 91-99.
- [40] C. M. Hindson, G. R. Hanson, P. S. Francis, J. L. Adcock, N. W. Barnett, *Chem. Eur. J.* **2011**, *17*, 8018-8022.
- [41] E. Kerr, E. H. Doeven, G. J. Barbante, C. F. Hogan, D. J. Hayne, P. S. Donnelly, P. S. Francis, *Chem. Sci.* **2016**, *7*, 5271-5279.
- [42] M. J. Frisch, G. W. Trucks, H. B. Schlegel, G. E. Scuseria, M. A. Robb, J. R. Cheeseman, G. Scalmani, V. Barone, B. Mennucci, G. A. Petersson, H. Nakatsuji, M. Caricato, X. Li, H. P. Hratchian, A. F. Izmaylov, J. Bloino, G. Zheng, J. L. Sonnenberg, M. Hada, M. Ehara, K. Toyota, R. Fukuda, J. Hasegawa, M. Ishida, T. Nakajima, Y. Honda, O. Kitao, H. Nakai, T. Vreven, J. J. A. Montgomery, J. E. Peralta, F. Ogliaro, M. Bearpark, J. J. Heyd, E. Brothers, K. N. Kudin, V. N. Staroverov, R. Kobayashi, J. Normand, K. Raghavachari, A. Rendell, J. C. Burant, S. S. Iyengar, J. Tomasi, M. Cossi, N. Rega, J. M. Millam, M. Klene, J. E. Knox, J. B. Cross, V. Bakken, C. Adamo, J. Jaramillo, R. Gomperts, R. E. Stratmann, O. Yazyev, A. J. Austin, R. Cammi, C. Pomelli, J. W. Ochterski, R. L. Martin, K. Morokuma, V. G. Zakrzewski, G. A. Voth, P. Salvador, J. J. Dannenberg, S. Dapprich, A. D. Daniels, Ö. Farkas, J. B. Foresman, J. V. Ortiz, J. Cioslowski, D. J. Fox, Gaussian, Inc., Wallingford CT, **2009**.
- [43] C. Adamo, V. Barone, *J. Chem. Phys.* **1998**, *108*, 664-675.
- [44] F. Weigend, R. Ahlrichs, *Phys. Chem. Chem. Phys.* **2005**, *7*, 3297-3305.
- [45] a) J. Lin, K. Wu, M. Zhang, *J. Comput. Chem.* **2009**, *30*, 2056-2063; b) R. V. Kiran, C. F. Hogan, B. D. James, D. J. D. Wilson, *Eur. J. Inorg. Chem.* **2011**, 4816-4825.
- [46] K. Nozaki, K. Takamori, Y. Nakatsugawa, T. Ohno, *Inorg. Chem.* **2006**, *45*, 6161-6178.
- [47] a) J. P. Perdew, K. Burke, M. Ernzerhof, *Phys. Rev. Lett.* **1996**, *77*, 3865-3868; b) J. P. Perdew, K. Burke, M. Ernzerhof, *Phys. Rev. Lett.* **1997**, *78*, 1396.
- [48] a) A. D. Becke, *Phys. Rev. A: Gen. Phys.* **1988**, *38*, 3098-3100; b) J. P. Perdew, *Phys. Rev. B* **1986**, *33*, 8822-8824.
- [49] C. Adamo, V. Barone, *J. Chem. Phys.* **1999**, *110*, 6158-6169.
- [50] A. D. Becke, *J. Chem. Phys.* **1993**, *98*, 5648-5652.
- [51] T. Yanai, D. P. Tew, N. C. Handy, *Chem. Phys. Lett.* **2004**, *393*, 51-57.
- [52] J.-D. Chai, M. Head-Gordon, *Phys. Chem. Chem. Phys.* **2008**, *10*, 6615-6620.
- [53] J. Tomasi, B. Mennucci, R. Cammi, *Chem. Rev.* **2005**, *105*, 2999-3093.
- [54] A. V. Marenich, C. J. Cramer, D. G. Truhlar, *J. Phys. Chem. B* **2009**, *113*, 6378-6396.
- [55] A. L. Tenderholt.
- [56] a) I.-S. Shin, Y.-T. Kang, J.-K. Lee, H. Kim, T. H. Kim, J. S. Kim, *Analyst* **2011**, *136*, 2151-2155; b) C. Li, S. Zhu, Y. Ding, Q. Song, *J. Electroanal. Chem.* **2012**, *682*, 136-140; c) M.-J. Li, Y.-Q. Shi, T.-Y. Lan, H.-H. Yang, G.-N. Chen, *J. Electroanal. Chem.* **2013**, *702*, 25-30; d) X. Ni, T. Li, Q. Song, *J. Electroanal. Chem.* **2014**, *719*, 30-34; e) Y. Liu, Q. Song, *Anal. Methods* **2014**, *6*, 5258-5263.
- [57] F.-R. F. Fan, in *Electrogenerated Chemiluminescence* (Ed.: A. J. Bard), Marcel Dekker, New York, **2004**, pp. 23-99.
- [58] J. K. Leland, M. J. Powell, *J. Electrochem. Soc.* **1990**, *137*, 3127-3131.



## Entry for the Table of Contents

## ARTICLE



**For future reference:** A re-examination of the co-reactant electrogenerated chemiluminescence (ECL) of Ir(C<sup>^</sup>N)<sub>2</sub>(acac) complexes shows that relative ECL intensity measurements (commonly used to evaluate the analytical utility of new electrochemiluminophores) can vary markedly depending on reaction conditions, and therefore can be overestimated if conditions disfavour the reference luminophore.

Lifen Chen, Egan H. Doeven,\* David J. D. Wilson, Emily Kerr, David J. Hayne, Conor F. Hogan, Wenrong Yang, Tien T. Pham, and Paul S. Francis\*

Page No. – Page No.

**Co-reactant electrogenerated chemiluminescence of iridium(III) complexes containing an acetylacetonate ligand**